Monitoring of Electromagnetic Environment along High-Speed Railway Lines Based on Compressive Sensing

Diego Bellan[*] **and Sergio A. Pignari**

Abstract—This paper deals with an efficient methodology aimed at monitoring the radiated electromagnetic emissions along a high-speed railway system in the hundreds of kilohertz range. In particular, the proposed approach allows a compressed representation of the spatial distribution of the frequency spectrum of the radiated magnetic field generated by the currents placed on the railway conductors by electrical apparatus on board of running railway vehicles. The main idea underlying this work is that the standing wave nature of current distribution along the railway line results in a spatial distribution of radiated magnetic field which can be effectively represented by resorting to the emerging compressive sensing theory. To this aim, wireless magnetic-field sensors are assumed to be deployed along the railway line and used to provide spatial samples of the magnetic field spectrum. The main advantages of the proposed approach include a smaller number of sensors when compared with the number foreseen by the straightforward use of the conventional Nyquist-Shannon sampling approach, and a simple treatment of nonuniform spatial distribution of sensors. Suitability of the proposed approach is supported by measurement data and electromagnetic models already available in the related literature, whereas effectiveness of field spatial reconstruction is proved through numerical simulations. Although the application presented in this work is specific to the magnetic field distribution in a limited frequency range, the proposed approach has a general validity and could be effectively exploited for distributed monitoring of other physical quantities, in other frequency ranges, related to electromagnetic compatibility and safety/security issues in high-speed railway systems.

1. INTRODUCTION

High-speed railway lines are complex systems from the structural, technological, and functional viewpoints. As a consequence, and in consideration of their impact and relevance to today's and future society, smart and optimized management of all the safety aspects related to high-speed lines is a mandatory and complex task. In this context, monitoring of the electromagnetic environment in proximity of high-speed railway lines is an important issue for both technical and health-risk evaluation reasons. Indeed, high levels of electrical power managed by modern railway systems together with operation of switching devices on board of rolling stock result in conducted emission (CE) of unwanted currents, mainly in the range of tens-hundreds of kilohertz, from the moving vehicle towards the railway line [1, 2]. Such currents represent the source of radiated emission (RE) of magnetic field along a railway system. A compressed representation of the spatial distribution of the magnetic field radiated by a railway system is the main objective of this paper. Nowadays, the availability of wireless sensors for magnetic/electric fields leads to the possibility to implement wireless sensor networks for monitoring wide areas such as railway lines. However, the main problem arising from the need of monitoring an area with large spatial extent is the huge amount of data to be acquired and processed. To face this problem, the paper proposes an innovative approach based on the emerging theory of Compressive

Sensing (CS) [3–12]. CS theory applies when the underlying signals of interest (in the time or in the space domain) exhibit a degree of sparsity, which means that in an appropriate basis they can be expressed in terms of a small number of nonzero coefficients with negligible information loss. For the specific application under analysis, the basic assumption is that the spatial distribution of the radiated magnetic field spectrum exhibits a proper degree of sparsity in the spatial frequency domain. This property stems from the standing wave pattern of CE current along the railway line and can be easily proven from previous works where both measurement data and modeling results have been reported [1, 13]. Thus, since the field spatial distribution is sufficiently sparse, it can be recovered from a number of observations smaller than the signal dimension, i.e., smaller than the number of samples required by the straightforward use of the conventional Nyquist-Shannon approach. It follows that the main advantage offered by CS in the given context is that the number of needed sensors can be much less than the number foreseen by the direct and blind implementation of the classical sampling theory. Moreover, since CS does not require uniform samples, spatial distribution of sensors is not required to be uniform. Finally, notice that even though the application presented in this work is specific to the magnetic field distribution in a limited frequency range, the proposed approach has a general validity and could be effectively exploited for distributed monitoring of other physical quantities, in other frequency ranges, related to electromagnetic compatibility and safety/security issues in high-speed railway systems.

The paper is organized as follows. In Section 2 the main concepts and background concerning CS theory are recalled. In Section 3 the main properties of the electromagnetic environment along a high-speed railway line are described, and the suitability of the CS approach is shown. In Section 4 numerical simulations are presented to validate the effectiveness of the CS approach in reconstructing spatial distributions of magnetic field spectrum along a railway line. Finally, concluding remarks are drawn in Section 5.

2. COMPRESSIVE SENSING AND FIELD RECONSTRUCTION

CS theory states that, under proper assumptions, a waveform can be reconstructed from a number of measurements (or samples) much smaller than the number of measurements required by conventional methods based on straightforward application of Shannon sampling theorem. CS theory is mainly based under two assumptions: a) Sparsity of the waveform to be reconstructed; b) Incoherence concerning the measurement (sensing) procedure. More specifically, sparsity exploits the property of most waveforms to be represented by a small number of coefficients when a proper basis Ψ is adopted, whereas incoherence refers to the property of a good sensing matrix Φ to be sufficiently incoherent to the basis Ψ under which the waveform is sparse [5].

The main idea underlying CS theory is therefore to provide a compressed representation of the waveform by implementing a measurement/sampling procedure (through the sensing matrix Φ) consisting in correlating the waveform with a small number of waveforms exhibiting a random behavior with respect to the sparsity basis Ψ (i.e., random projections). Thus, CS is a procedure performing simultaneously and efficiently both sensing and compression of the waveform, moving the main computational burden to the subsequent procedure of waveform recovery.

2.1. Field Sampling

The approach proposed in this paper foresees both time and space sampling. Time sampling is operated through the conventional approach, whereas space sampling will take advantage of CS theory. More specifically, it is assumed that each sensor operates in the time domain by sampling the component of the magnetic field parallel to the ground and orthogonal to the railway line. The distance to the rails is prescribed by the related Standards [1]. Then the time samples are transformed into the frequency domain through the well-known Fast Fourier Transform. Thus, for each measurement time window, each sensor provides the frequency spectrum at the related sensor location. The spatial distribution of the magnitude of each frequency component of interest represents the space waveform to be sampled and reconstructed through the CS approach.

Let us consider a discrete waveform $f \in \mathbb{R}^n$ in the spatial domain representing the spatial distribution of a spectral component of the field under analysis. The measurement/sampling procedure

can be described by the linear functional transformation:

$$y_k = \langle f, \varphi_k \rangle = \varphi_k^T f, \quad k = 1, \ldots, m \tag{1}$$

where m is the number of signal measurements, and $\{\varphi_k\}_{k=1}^m$ are the measurement waveforms. In (1) the field f is thus correlated with the measurement waveforms $\{\varphi_k\}_{k=1}^m$. As an important special case, exploited in the present work, if the measurement waveforms $\{\varphi_k\}_{k=1}^m$ are Dirac's delta functions then the measured vector y consists of the samples of the field f.

In the following we are interested in the undersampling problem, i.e., the case where the number m of measurements is much smaller than the dimension n of the signal. This circumstance is important from a practical viewpoint since it corresponds to the case where the number of available field sensors is limited with respect to the dimension of the field spatial distribution to be measured and recovered.

If Φ denotes the measurement matrix consisting of the row vectors $\{\varphi_k^T\}_{k=1}^m$ of the measurement waveforms, the vector of the measured values can be written as

$$y = \Phi f \tag{2}$$

where $y \in \mathbb{R}^m$ with $m < n$. Notice that there exist infinitely many solutions $\tilde{f} \in \mathbb{R}^n$ that give rise to $\Phi \tilde{f} = y$. Under the assumptions of sparsity and incoherence, however, CS theory provides one solution of (2).

Moreover, notice that actual measurements are always affected by noise. Thus, in order to evaluate the impact of noise on the reconstructed field, an additive noise term u should be added in (2) to provide the analytical description of noise contribution:

$$y = \Phi f + u \tag{3}$$

2.2. Sparsity and Incoherence

It is assumed that the field f can be represented in a proper orthonormal basis $\Psi = [\psi_1 \psi_2 \ldots \psi_n]$. Thus, the k-th field component f_k can be written as

$$f_k = \sum_{i=1}^n x_i \psi_{ik} \tag{4}$$

where $x_i = \langle f, \psi_i \rangle = \psi_i^T f$, and the vector field f can be written as

$$f = \Psi x \tag{5}$$

In this work, by taking into account the electromagnetic environment described in Section 3, the trigonometric Fourier basis will be adopted, i.e.,

$$f = \begin{bmatrix} f_1 \\ f_2 \\ \vdots \\ f_n \end{bmatrix} = \Psi x = \begin{bmatrix} 1_n & \psi_{c,1} & \psi_{c,2} & \cdots & \psi_{c,(n-1)/2} & \psi_{s,1} & \psi_{s,2} & \cdots & \psi_{s,(n-1)/2} \end{bmatrix} \begin{bmatrix} a_0 \\ a_1 \\ a_2 \\ \vdots \\ a_{(n-1)/2} \\ b_1 \\ b_2 \\ \vdots \\ b_{(n-1)/2} \end{bmatrix} \tag{6}$$

where

$$\psi_{c,k} = \begin{bmatrix} \cos\left(2\pi k \cdot \frac{0}{n}\right) \\ \cos\left(2\pi k \cdot \frac{1}{n}\right) \\ \vdots \\ \cos\left(2\pi k \cdot \frac{n-1}{n}\right) \end{bmatrix}, \quad \psi_{s,k} = \begin{bmatrix} \sin\left(2\pi k \cdot \frac{0}{n}\right) \\ \sin\left(2\pi k \cdot \frac{1}{n}\right) \\ \vdots \\ \sin\left(2\pi k \cdot \frac{n-1}{n}\right) \end{bmatrix} \tag{7}$$

and 1_n is a column vector consisting of ones.

A waveform is characterized by sparsity S when it can be represented, with negligible information loss, by its largest S coefficients x_i and by neglecting (i.e., by assuming equal to zero) the remaining coefficients. By denoting as x_S the vector consisting of the largest S coefficients and setting equal to zero the remaining coefficients, we obtain the strict-sense sparse vector:

$$f_S = \Psi x_S \tag{8}$$

which provides an approximation to the field f. Since Ψ is an orthonormal basis,

$$\|f - f_S\|_{l_2} = \|x - x_S\|_{l_2} \tag{9}$$

it follows that if x is well approximated by x_S then the error $\|f - f_S\|_{l_2}$ is small.

Incoherence can be fulfilled by selecting a random sensing matrix Φ. An interesting choice for the application under analysis is $\varphi_k(z) = \delta(z - k)$, consisting in Dirac's delta functions placed at sensor locations. By selecting the Fourier basis as Ψ, the well-known sampling scheme is obtained. It can be shown [5] that this choice corresponds to the maximal incoherence between Φ and Ψ, not just in one dimension but in any dimension. Moreover, it is interesting to notice that a uniform sensors displacement is not required for the adopted sampling scheme. This could be a very advantageous point in practical applications where uniform displacement of sensors is not feasible or some sensors are not functioning.

2.3. Field Reconstruction

Given the m measurements in (1), CS theory states that the sparsest Fourier representation of the field, consistent with measurements, can be recovered by ℓ_1-norm minimization of a vector $\tilde{x} \in \mathbb{R}^n$ subject to $y_k = \langle \tilde{f}, \varphi_k \rangle = \langle \Psi \tilde{x}, \varphi_k \rangle$, i.e., [5]:

$$\min_{\tilde{x} \in \mathbb{R}^n} \|\tilde{x}\|_{\ell_1} \quad \text{subject to} \quad y_k = \langle \Psi \tilde{x}, \varphi_k \rangle, \quad k = 1, \ldots, m \tag{10}$$

where $\|x\|_{l_1} = \sum_i |x_i|$. It means that among all the objects $\tilde{f} = \Psi \tilde{x}$ consistent with the measurement data, the selected object is the one whose sequence of Fourier coefficients is the sparsest and minimizes the norm ℓ_1.

It can be shown that, under the assumption of incoherence, if the number of measurements m is such that

$$m \geq CS \log n \tag{11}$$

with C a positive constant, then the solution is exact with overwhelming probability.

Notice that the required number of measurements is of the order of $S \log n$, therefore for a given sparsity S the required number of measurements m increases with the signal length n. It means that for proper signal reconstruction a degree of redundancy is required, i.e., a number of measurements m greater than the signal sparsity S is necessary. This is the price to pay in order to recover spectral components whose location on the frequency axis is unknown [12]. This point must be taken into account when a comparison with the Nyquist-Shannon approach is performed. In fact, while theoretical signal compression is n/S, the CS compression factor is n/m, i.e., the actual CS compression is lower than the theoretical one [12]. Many researchers have put into evidence the practical rule $m = 4S$ for m selection. However, from (11) and the results in [12] it is clear that this is only an empirical rule, which holds in many practical cases according to the weak logarithmic dependence from the signal length n. A more accurate and explicit law for m selection is reported in [12]. Finally, it is worth noticing that the minimum number of measurements has a probabilistic meaning, i.e., a small number of measurements could result in a high probability to pick particular signal values that do not allow proper signal recovery.

3. ELECTROMAGNETIC ENVIRONMENT ALONG A RAILWAY SYSTEM

Modern high-speed railway systems consist of electrical apparatus involving high power levels and switching technology for energy conversion. A moving train, in particular, can be seen as a moving source of electrical disturbances injected into the railway system through the contact line. Such disturbances, in the form of electrical currents with frequency spectra extended typically to several hundreds of kilohertz, propagate along the horizontal conductors of the railway system (i.e., the contact line, the feeder, the

rails, and the ground wires) which, in turn, behave as horizontal antennas generating electromagnetic field. Measurement techniques for radiated electromagnetic emissions from a railway system have already received attention in the technical literature. A standard technique foresees measurement of the radiated field in a given measurement point along the railway line while the train is moving and passing in front of such point. However, since the electromagnetic field is generated by the whole railway system acting as an antenna as mentioned above, the maximum electromagnetic field is not measured when the train is in front of the measurement point, but it could be measured when the train is a few kilometers away from such point.

A much more complete characterization of the electromagnetic field radiated by a railway system could be attained by placing electromagnetic field sensors along the whole railway line to provide a proper spatial sampling of the field such that the field spatial distribution can be reconstructed. To this aim, the CS theory recalled in Section 2 is very well suited for two main reasons. First, it is reasonable to assume that the spatial behavior of the radiated field along a railway line has a sparse representation in the spatial frequency domain. This point is closely related to the standing wave behavior of the current injected into the railway line and it can be observed in Figures 1 and 2 where a typical spatial distribution of the radiated magnetic field along a railway line 16 km in length and with the train in position 4 km is shown. The figures have been obtained by means of a simplified model of a high-speed railway line [13] showing a good agreement with more complex simulation models and with measurement data [1]. In particular, in Figure 1 it is clear that by increasing the frequency from 60 kHz to 150 kHz (vertical axis) the spatial distribution of the field increases its spatial frequency as well (i.e., spatial maxima are closer each other). In Figure 2, as an example, the spatial distribution of the magnetic field at 94 kHz and 141 kHz is shown. The spatial behavior is mainly consisting of a mean value and a sine wave component. Notice that higher field frequency results in higher spatial frequency. It is of paramount importance to notice that with the conventional Nyquist-Shannon approach, by increasing the spatial frequency a larger number of sensors would be required for proper sampling. On the contrary, thanks to the sparsity assumption, the CS approach does not require an increasing number of sensors because the sparsity degree does not change.

The second reason for which CS is well suited to the problem at hand is that uniform placing of sensors along the railway line is not required. In fact, uniform deployment of sensors could be not practical in many situations. In other cases, some sensors could be not functioning. Indeed, uniform sensor deployment is not required by the CS approach.
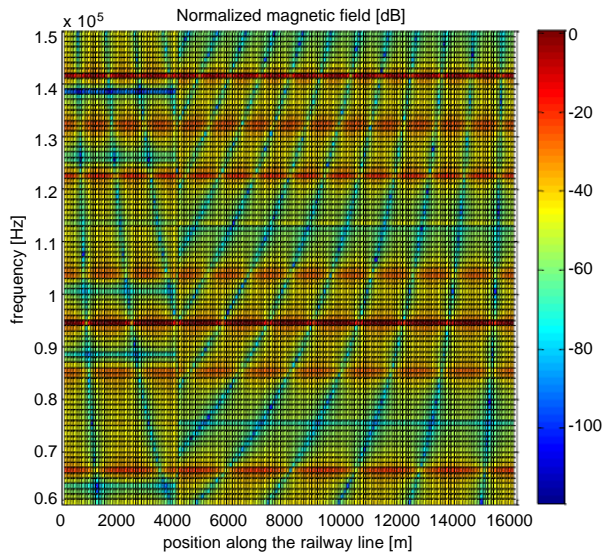

Figure 1. Typical space-frequency distribution of magnetic field along a simulated high-speed railway line 16 km in length. The train position is at 4 km.
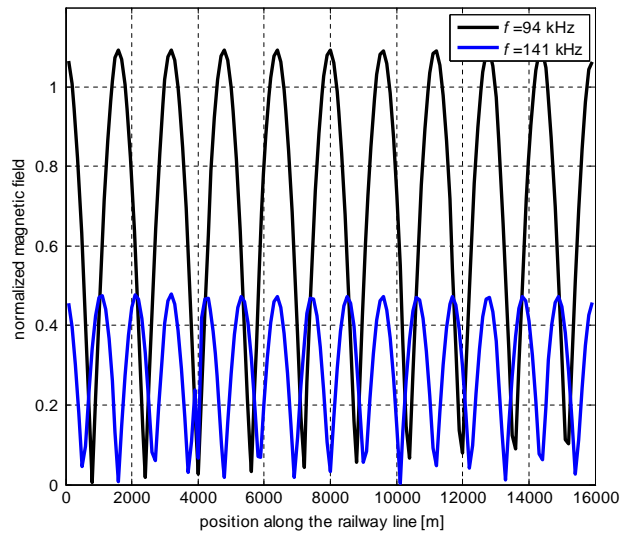

Figure 2. Spatial distribution of the magnetic field along the simulated railway line considered in Figure 1, for two specific frequencies, i.e., $f = 94$ kHz (black line) and $f = 141$ kHz (blue line).

4. NUMERICAL VALIDATION

Field reconstruction based on the CS approach reported in Section 2 was validated within the application context outlined in Section 3. In particular, as a specific example, the main objective was the assessment of CS capability in the reconstruction of the field spatial distributions reported in Figure 2. The frequencies in Figure 2 were selected since they correspond to strong frequency components in Figure 1. However, the same validation could be performed for any frequency component of the magnetic field. The main parameter to be selected for numerical validation is the number of sensors m, i.e., the number of samples (or number of measurements) of the field to be reconstructed. The value $m = 20$ was selected according to the practical rule of $4S$ mentioned at the end of Section 2. Indeed, according to the practical rule, the choice $m = 20$ corresponds to a sparsity $S = 5$, i.e., the CS algorithm will provide the largest 5 Fourier coefficients in the model (6). This seems to be a reasonable choice for spatial distributions like those shown in Figure 2, since further Fourier components other than the mean value and the fundamental sinewave component are needed to recover only the waveform details such as discontinuity at train position and the sharp behavior at the waveform bottom part. A more accurate selection of m requires the specification of the waveform length n according to redundancy recalled in Section 2. A reasonable choice for n is 160 (i.e., one sample per 100 meters along the 16-km line) since with the conventional Nyquist-Shannon approach and by taking into account the current standing wave distribution, the corresponding maximum frequency of the field to be measured would be 750 kHz, i.e., a frequency range including the range of practical interest. According to [12], the relative sparsity $S/n = 5/160$ corresponds to a degree of redundancy $m/S \approx 4$, i.e., the same value provided by the practical rule mentioned above. Therefore the selected number of sensors is $m = 20$. The locations of the m sensors are selected at random within the length of the considered railway line. In Figure 3 the field spatial distribution corresponding to $f = 94$ kHz (i.e., the black line in Figure 2) is plotted together with a typical distribution reconstructed through the CS approach (red line). Notice that the conventional Nyquist-Shannon approach would lead to an aliased reconstruction of the field since the number of periods in Figures 3 is 10, whereas the number of uniform samples would be $m = 20$. Moreover, notice that since the locations of the m sensors were selected randomly, repeated simulation
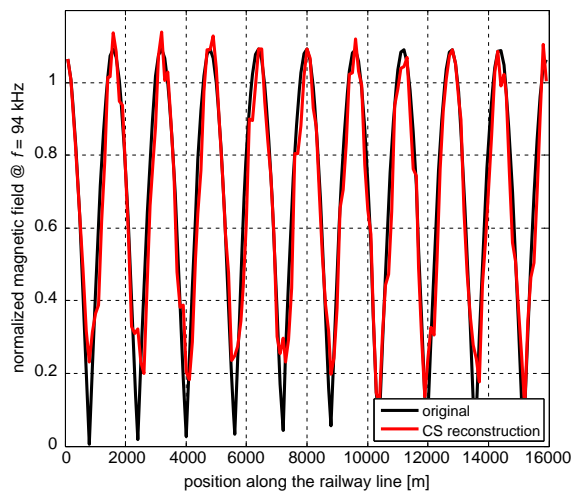

Figure 3. Comparison between the original behavior (black line) of the magnetic field along the simulated railway line at $f = 94$ kHz (also represented by the black line in Figure 2) and the reconstructed field by means of the CS theory approach (red line). The number of sensors randomly distributed along the line is 20.
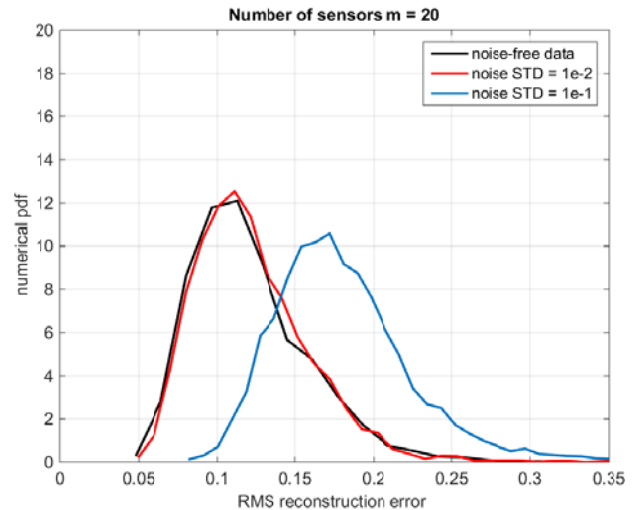
Figure 4. Numerically estimated pdf of the RMS reconstruction error for the same field in Figure 3 ($f = 94$ kHz). Repeated run analysis (5000 runs) was performed with $m = 20$ sensors with random locations. Additive Gaussian noise effect was also considered (red and blue lines).

runs will provide slightly different behaviors. For each simulation run the RMS reconstruction error can be evaluated. In Figure 4 the estimated probability density function (pdf) of the RMS reconstruction error obtained through 5000 repeated runs is shown. The black line shows the noise-free case, while the red and blue lines refer to independent additive Gaussian noise with zero mean and standard deviation (STD) 10^{-2} and 10^{-1} respectively. Notice that the peak-to-peak amplitude of the field in Figure 3 is about 1. The main source of noise in a practical implementation can be ascribed to analog-to-digital (ADC) conversion of sensor signals. Notice that due to the need of reducing the amount of data to be processed, low-resolution ADCs are required. In this case it is well known that quantization effects can heavily affect the acquired data [9, 14–18], therefore the investigation of noise impact is of paramount importance. In Figure 4 the noise level 10^{-2} clearly has no substantial effect, whereas the noise level 10^{-1} has a significant effect. In Figure 5 the numerical pdf of the RMS reconstruction error has been estimated for a larger number of sensors, i.e., $m = 25$. A higher accuracy of the reconstructed field was obtained since a larger number of Fourier coefficients was recovered by the algorithm. In fact, since the waveform to be reconstructed is not sparse in a strict sense, the assumed sparsity S implies that the other Fourier coefficients are neglected in the reconstruction.

Figure 6 compares the original and the CS reconstructed fields for the frequency $f = 141\,\text{kHz}$ (i.e., the blue line in Figure 2) and $m = 20$. The same remarks as for Figure 3 hold in this case. In Figure 6 a third line (i.e., the blue line) is reported, corresponding to the reconstructed field by means of the conventional Nyquist-Shannon approach based on uniform sampling. Notice that since the number of samples is $m = 20$, and the number of the original field periods in Figure 6 is 15, aliasing is clearly apparent. Of course, it results in a completely wrong reconstruction of the field. This is a key advantage of the proposed CS approach. In fact, while the Nyquist-Shannon approach would require an increasing number of (equally spaced) measurement points for increasing spatial frequency of the field to be reconstructed, the CS approach requires a constant number of measurement points provided that the field sparsity does not change.
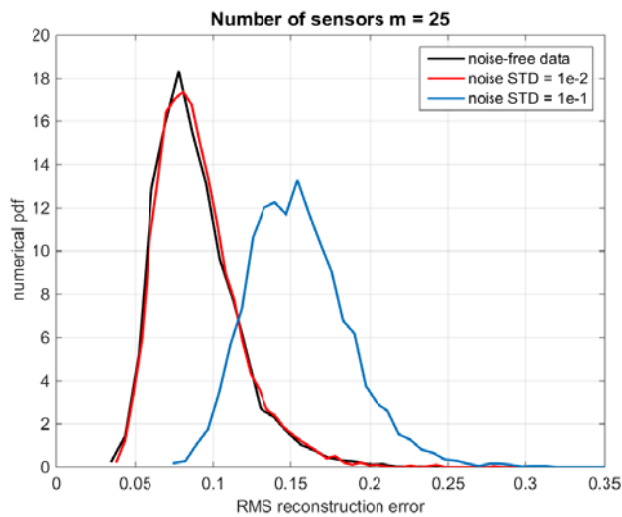

Figure 5. Numerically estimated pdf of the RMS reconstruction error for the same field in Figure 3 ($f = 94\,\text{kHz}$). Repeated run analysis (5000 runs) was performed with $m = 25$ sensors with random locations. Additive Gaussian noise effect was also considered (red and blue lines).
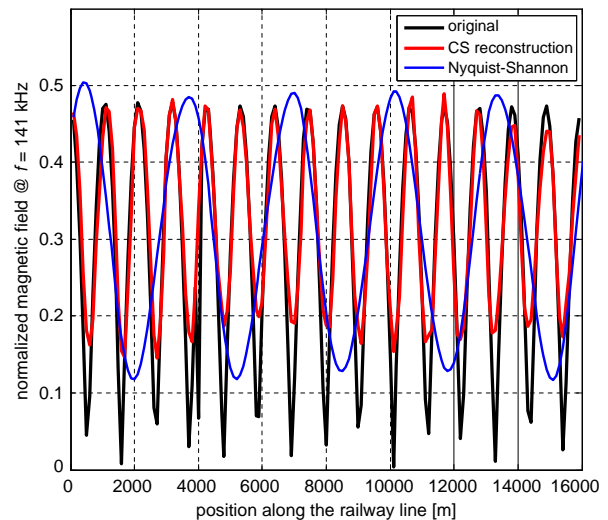
Figure 6. Comparison between the original (black line) and the CS-reconstructed (red line) magnetic field at $f = 141\,\text{kHz}$ along the simulated railway line with $m = 20$. The blue line shows the reconstructed field by means of the conventional Nyquist-Shannon theorem, resulting in an aliased reconstruction due to a number of sensors smaller than required by such theorem.

5. CONCLUSION

In the paper, it was proven that CS theory is very well suited for reconstruction of radiated magnetic field along a high-speed railway line. It was shown that this is mainly due to the fact that a typical space distribution of each magnetic-field frequency component has a sparse representation in the spatial frequency domain since it is closely related to the standing wave nature of the corresponding current. This feature results in a required number of sensors much lower than that required according to the straightforward application of the conventional Nyquist-Shannon approach. This advantage becomes more and more evident as the frequency of the magnetic field to be reconstructed increases. Moreover, CS theory does not require a uniform distribution of sensors. This is of paramount importance in a practical implementation of the proposed approach, since uniform distribution often cannot be attained in a real railway system.

REFERENCES

1. Bellan, D., G. Spadacini, E. Fedeli, and S. A. Pignari, "Space-frequency analysis and experimental measurement of magnetic field emissions radiated by high-speed railway systems," *IEEE Trans. Electromagn. Compat.*, Vol. 55, No. 6, 1031–1042, 2013.
2. Bellan, D., A. Gaggelli, F. Maradei, A. Mariscotti, and S. A. Pignari, "Time-domain measurement and spectral analysis of nonstationary low-frequency magnetic-field emissions on board of rolling stock," *IEEE Trans. Electromagn. Compat.*, Vol. 46, No. 1, 12–23, 2004.
3. Candès, E. J., J. Romberg, and T. Tao, "Robust uncertainty principles: Exact signal reconstruction from highly incomplete frequency information," *IEEE Trans. Inf. Theory*, Vol. 52, No. 2, 489–509, 2006.
4. Candès, E. J. and T. Tao, "Near-optimal signal recovery from random projections: Universal encoding strategies?" *IEEE Trans. Inf. Theory*, Vol. 52, No. 12, 5406–5425, 2006.
5. Candès, E. J. and M. B. Wakin, "An introduction to compressive sampling," *IEEE Signal Processing Magazine*, Vol. 25, No. 2, 21–30, 2008.
6. Tropp, J. A., J. N. Laska, M. F. Duarte, J. K. Romberg, and R. G. Baraniuk, "Beyond Nyquist: Efficient sampling of sparse bandlimited signals," *IEEE Trans. Inf. Theory*, Vol. 56, No. 1, 520–544, 2010.
7. Dong, M., L. Tong, and B. M. Sadler, "Impact of data retrieval pattern on homogeneous signal field reconstruction in dense sensor networks," *IEEE Trans. Signal Process*, Vol. 54, No. 1, 4352–4364, 2006.
8. Yang, A. Y., M. Gastpar, R. Bajcsy, and S. Shankar Sastry, "Distributed sensor perception via sparse representation," *Proc. of the IEEE*, Vol. 98, No. 6, 1077–1088, 2010.
9. Bellan, D., "Reconstruction of noisy electromagnetic fields by means of compressive sensing theory," *Applied Mechanics and Materials*, Vols. 263–266, 99–102, 2013.
10. Wang, P. Y., Q. Song, and Z. M. Zhou, "A physics-based landmine discrimination approach with compressive sensing," *Progress In Electromagnetics Research*, Vol. 135, 37–53, 2013.
11. Xia, S., Y. Liu, J. Sichina, and F. Liu, "A compressive sensing signal detection for UWB radar," *Progress In Electromagnetics Research*, Vol. 141, 479–495, 2013.
12. Yaroslavsky, L., "Is 'compressed sensing' compressive? Can it beat the Nyquist sampling approach?" *Physics. Optics cs. IT Math. IT*, arXiv: 1501.01811v2, Jan. 9, 2015.
13. Bellan, D., G. Spadacini, F. Grassi, E. Fedeli, and S. A. Pignari, "Modeling strategies for conducted and radiated emissions in high-speed railway lines," *Proceedings of Asia-Pacific Int. Symp. on Electromagn. Compat. (APEMC 2013)*, 288–291, Melbourne, Australia, May 20–23, 2013.
14. Bellan, D., A. Brandolini, and A. Gandelli, "Quantization theory in electrical and electronic measurements," *Proc. 1995 IEEE Instrumentation and Measurement Technology Conference*, 494–499, Waltham, MA, USA, Apr. 23–26, 1995.

15. Bellan, D., A. Brandolini, L. Di Rienzo, and A. Gandelli, "Improved definition of the effective number of bits in ADC testing," *Computer Standards and Interfaces*, Vol. 19, Nos. 3–4, 231–236, 1998.

16. Bellan, D., A. Brandolini, and A. Gandelli, "ADC nonlinearities and harmonic distortion in FFT test," *Proc. 1998 IEEE Instrumentation and Measurement Technology Conference*, 1233–1238, St. Paul, MN, USA, May 18–21, 1998.

17. Bellan, D., "Model for the spectral effects of ADC nonlinearity," *Measurement: Journal of the International Measurement Confederation*, Vol. 26, No. 2, 65–76, 2000.

18. Bellan, D., "On the validity of the noise model of quantization for the frequency-domain amplitude estimation of low-level sine waves," *Metrology and Measurement Systems*, Vol. 22, No. 1, 89–100, 2015.